The study of electro-optical properties of nanocomposite ITO thin films prepared by e-beam evaporation

M. Farahamndjou
Department of physics, Varamin Pishva Branch, Islamic Azad University, Varamin, Iran,
Tel: +982136725011-14,
e-mail: farahmandjou@iauvaramin.ac.ir

Received 17 September 2012; accepted 6 February 2013

Indium-tin oxide thin films are deposited on sods lime glass substrates using e-beam evaporation system. In order to improve the structural, electrical and optical properties of the films, these films were annealed in vacuum and different temperature. The structure, sheet resistance and optical transmission of the films were systematically investigated as function of post annealing temperature. It has been observed that the films take its maximum transmission and conductivity at annealing temperature 400°C. The XRD and AFM analysis reveals that the amorphous films were oriented to $\langle 222 \rangle$ crystal texture direction with size of grains about 35-40 nm.

Keywords: ITO Nano-composite; crystallity; optical transmission; Thin Films.

PACS: 73.63.Bd; 78.67.Bf; 78.67.Sc

1. Introduction

Indium-tin oxides are the most widely used transparent conducting oxides for flat panel displays, primarily because they have high optical transmittance in the visible region, high electrical conductivity, surface uniformity and process compatibility [1]. Indium tin oxide (ITO) films are transparent electrical conductor used for optoelectronic devices because they have low resistivity and high transmittance in the visible region with an n-type degenerated semiconductor and a wide energy band (Eg $\approx$ 4 eV) [2]. Sn-doped In_2O_3 (ITO) is of great importance in technology and is widely used in electronic and optoelectronic devices due to its excellent electro-optical properties such as high electrical conductivity, transparency to light, high substrate adherence, good hardness, and chemical inertness [1-3]. ITO has the same two crystal structures as pure In_2O_3 [4], the bixbyite structure and the corundum structure [5]. Compared to the ITO with bixbyite structure, the ITO with corundum structure has some advantages such as higher specific gravity, higher green density, and more stable conductivity [6], which are favorable for its applications. Among all of the investigations on ITO, the research on its thin films has been the most interesting issue for several decades due to the applications in various fields such transparent electrodes for display devices, transparent coatings for solar energy heat mirrors, windows films, etc [7-9].

To satisfy the requirements of the wide applications of ITO thin films, a lot of research efforts have been made on the preparation of ITO films, and various manufacturing techniques such as reactive electron vaporation [9], D.C. and r.f. magnetron sputtering [10,11], reactive thermal deposition [12], laser ablation [13], spray pyrolysis [14], and sol-gel process [15] have been successfully developed. Especially in recent years, the sol-gel method has been considered as one of the best available processes, and has been fully investigated. It has been seen that the structure, electrical and optical properties of the ITO films are strongly affected by deposition steps and one can improve these properties by post annealing after deposition [16].

In this work, Indium-tin oxide thin films are first deposited on sods lime glass substrates by e-beam evaporation in room temperature and then annealed at different temperature. The structural, electrical and optical properties of the nanocomposite ITO films have been studied in different annealing temperature.

2. Experimental method

The ITO films were prepared by electron evaporation on glass substrate at room temperature using an ITO target composite of mixture of 90 wt% In_2O_3 and 10 wt% SnO_2 99.99% purity. The glass substrates were ultrasonically cleaned in an acetone and de-ionized water before depositions. The films were deposited at a base pressure of 8×10^{-6} torr with deposition rate of 0.2 nm/s. After deposition process, the layers were annealed in different temperature for 1 hour.

The surface morphology of the thin film samples on a small scale was obtained using an atomic force microscopy (AFM) instrument in contact mode. AFM image were acquired, in ambient air, in constant force mode and digitized into 512×512 pixels. A variety of scans were acquired at random locations on the film surface. To analyze the AFM images, the topographic image data were converted into ASCII data. To determine the structure of films, the XRD measurement were performed using a Seifert with Cu-Kα radiation (wavelength = 1.54 A°). A Varian-Cary system 500 UV-Vis-NIR spectrophotometer was used to determine the optical transmission spectra.

3. Results and discussion

Figure 1 shows the effect of annealing temperature at 400°C for 1 hour on crystal structure of the ITO films. It could be

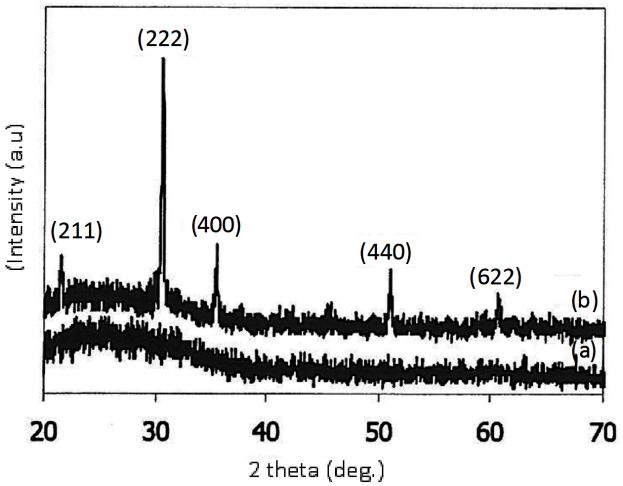

FIGURE 1. XRD spectra of ITO films (a) before and (b) after annealing at 400°C.

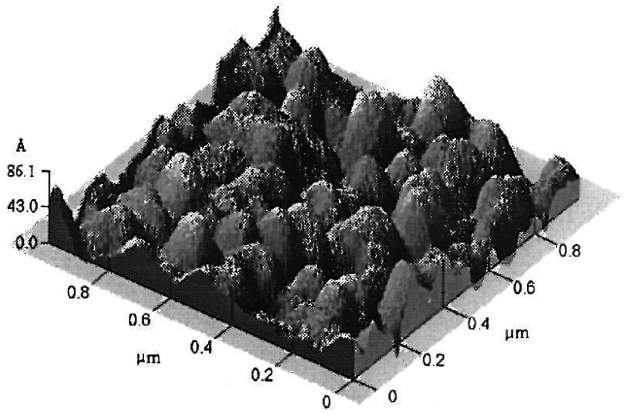

FIGURE 2. AFM images of ITO film after annealing at 400°C

seen from the Fig. 1(a) that the XRD pattern of as-deposited ITO film is amorphous. After annealing at the temperature of 400°C the ITO films show the XRD peak with intensities of the five major peaks, (211), (222), (400), (440) and (622). These picks show the cubic structure [17]. The crystallity increases as a function of annealing temperature. The XRD results show that the intensity (222) peak is higher when the ITO film annealed in vacuum at higher temperature. The structure of ITO film is rearranged by heating process and amorphous ITO film is then improved crystalline structure, due to annealing processes. The intensity ratio of I_{222}/I_{400} of ITO powder is about 3.33 [18].

According to Table I, the amorphous films are originated in $\langle 100 \rangle$ texture direction before annealing and the films are originated in $\langle 222 \rangle$ crystal texture direction after annealing. Especially the intensity ratio of I_{222}/I_{400} is too low at temperature of 400°C and the films are originated in $\langle 111 \rangle$ texture direction. As you can see from the table 1 the sheet resistance and optical transmission of the films is optimum in temperature of 400°C. The electrical conductivity is related to the number and mobility of carriers. In case of ITO grains when Sn atoms are substituted to indium atoms, an extra electron is injected to the atomic structure as free electron. Therefore oxygen vacancies add two free electrons to the structure and it increases the conductivity and decrease the sheet resistance. On the other hand by increasing of the crystallity of the ITO films the light scattering decreases and the optical transmission increases. In fact increasing the carriers cause to increasing the scattering and then decreasing the transmission. In fact, indium oxide containing intrinsic oxygen vacancies is an anion-deficient n-type conductor where the oxygen vacancy population limits the electron concentration. This deficiency persists the growth conditions, at high-temperature. With tin doping a charge imbalance is created due to the different valences of indium and tin. The charge imbalance can be compensated by incorporation of interstitial oxygen atoms or/and oxygen vacancies. Tin cations and interstitial oxygen anions can form cluster defects.

The standard atomic planar distance of 222, is d_{222}=2.921 A° for ITO films. In table 1 it can be seen that atomic planar distance of 222 is more than standard value before and after annealing. It shows that there is a stress in the layer which cause to a strain in the film because of heat expansion difference between glass substrate and ITO films [19]. According to XRD analysis with sheerer formula [20] and also with AFM picture the size of ITO grains are measured about 20 nm in $\langle 400 \rangle$ direction and grains are determined about 27-35 nm in $\langle 222 \rangle$ direction at 400°C.

Figure 2 show the AFM images of ITO thin films deposited on a glass substrate on the as-deposited film and after annealing at 400°C. The size of ITO grains is about 35-40 nm in $\langle 222 \rangle$ direction.

Figure 3 shows the UV-Vis-NIR transmission spectra before and after annealing at 400°C. It can be seen a decreasing in transmission in near IR region because of increasing of the carriers after annealing process [21].

TABLE I. Electro-optical and structural properties of ITO films.

Annealing circumstance	I_{222}/I_{400}	Atomic Planar Distance (222)	sheet resistance	Transmission (%)
Without annealing	Amorphous	Amorphous	17	23
200°C	0.13	2.981	300	82
300°C	0.50	2.980	91	81
400°C	0.33	2.955	16	85
450°C	0.66	2.960	44	85

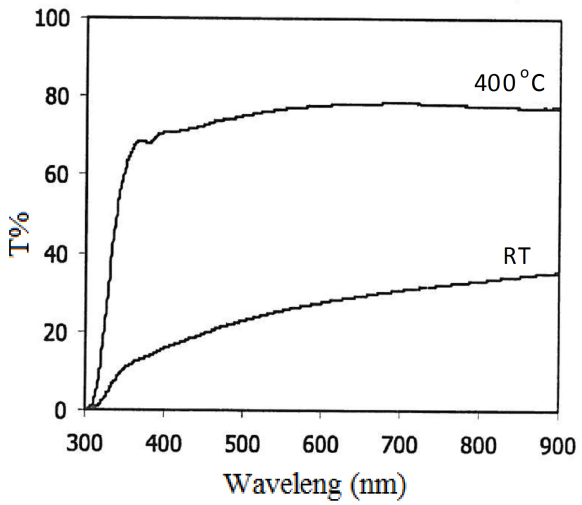

FIGURE 3. Shows the UV-Vis-NIR transmission spectra before and after annealing at 400°C. It can be seen a decreasing in transmission in near IR region because of increasing of the carriers after annealing process [21].

4. Conclusion

The structural, electrical and optical properties of the nanocomposite ITO films on sods lime glass substrates were studied in different annealing temperature. The results reveal that the size and crystallity of the ITO grains increase with annealing temperature and the films are oriented to $\langle 222 \rangle$ crystal texture direction at optimum 400°C with size of 35-40 nm.

Acknowledgments

The author is thankful for the financial support of Karaj material and energy research center for analysis and the discussions on the results.

1. I. Hambergend and C.G. Granquist, *J. Appl. Phys*. **60** (1986) 123.
2. Y. Dijaoued, V.A. Phong, S. Balidescu, P.V. Asrit, E.F. Girouard, and Z.V.V. Truong, *Thin Solid Films*. **293** (1997) 108.
3. D.M. Mattox, *Thin Solid Films*. **204** (1991) 25.
4. N. Nadaud, N. Lequeux, and M. Nanot, *J. Solid State Chemistry.* **135** (1998) 140.
5. R.D. Shannon, D.B. Rogers, and A.W. Sleight, *Inorg. Chem.* **8** (1969) 1985.
6. H.T. Akao, R. Suzuki, M. Tomoda, S. Tsukidate, and K. Fujita, *European Patent*. **2** (1999) 0921099.
7. H. Kim A. Piqué, J.S. Horwitz, H. Mattoussi, H. Murata, Z.H.. Kafafi, D.B. Chrisey, *Appl. Phys. Lett*. **74** (1999) 3444.
8. H. Hiramateu, W.S. Seo, and K. Koumoto, *Chem. Mater*. **10** (1998) 3033.
9. I.A. Rauf, R. F. Egerton, and M. Sayer, *J. Appl. Phys*. **79** (1996) 4057.
10. Y. Shigesato and D.C. Paine, *Thin Solid Films*. **238** (1994) 44.
11. F-El Akkad, A. Punnooze, and G. Prabu, *Appl. Phys. A.* **71** (2000) 157.
12. P. Thilakan, S. Kalainathan, J. Kumar, and P. Ramssamy, *J. Electron Mater.* **24** (1995) 719.
13. C. Cali, M. Mosa, and G. Taragia, *Solid State Electron* **42** (1998) 877.
14. M. Rami, E. Benamar, C. Messaoudi, D. Sayah, and A. Ennaoui, *Europian J. Solid State Inorganic Chem* **35** (1998) 211.
15. S.S. Kim, S.Y. Choi, C.G. Park, and H. Woo Jin, *Thin Solid Films* **347** (1999) 155.
16. H.Y. Yeom, N. Popovich, E. Chason, and D.C. Paine, *Thin Solid Films* **411** (2002) 17.
17. P. Thilakan, C. Minarini, S. Loreti, and E. Terzini, *Thin Solid Films* **388** (2001) 34.
18. C. Guillen and J. Herrero, *Thin Solid Fims* **510** (2006) 260.
19. C. Guillen and J. Herrero, *Thin Solid Fims* **480** (2005) 129.
20. A.E. Hichou, A. Kachouane, and J. L. Budendorff, *Thin Solid Fims* **458** (2004) 184.
21. C. Guillen and J. Herrero, *Thin Solid Fims* **431** (2003) 403.